Quantum transitions in Lennard-Jones clusters

Jason Deckman, Pavel A. Frantsuzov, and Vladimir A. Mandelshtam
Chemistry Department, University of California at Irvine, Irvine, California 92697, USA
(Received 10 February 2008; published 21 May 2008)

The ground states of Lennard-Jones (LJ) clusters are estimated by finding the Gaussian wave packets that minimize the energy functional. A "phase diagram" for LJ_n as a function of size ($n=31,\ldots,45$) and de Boer quantum delocalization length ($\Lambda\in[0;0.3]$) is constructed, showing the stability ranges for the two competing structural motifs, the Mackay and anti-Mackay icosahedra. An increase of Λ has an effect similar to heating and as such may induce structural transformations.

DOI: 10.1103/PhysRevE.77.052102 PACS number(s): 64.60.−i, 36.40.−c, 64.70.−p

Quantum effects play an important role in the dynamics and thermodynamics of many-body systems that include sufficiently light particles. However, due to the computational difficulties, the majority of studies of complex systems, e.g., Van der Waals clusters, are restricted to purely classical models. Therefore, understanding and quantification of quantum effects remains a big challenge in the fields of molecular dynamics and statistical mechanics simulations.

In the present study, we consider the commonly used model that represents a Van der Waals cluster by n particles interacting with each other via the Lennard-Jones (LJ) pair potential,

$$U(r_{ij}) = 4\epsilon[(\sigma/r_{ij})^{12} - (\sigma/r_{ij})^{6}]. \quad (1)$$

After using the reduced units for temperature (k_BT/ϵ), distance (r/σ), and energy (E/ϵ), a quantum monatomic LJ system is characterized by a single parameter, e.g., the de Boer quantum delocalization length $\Lambda=(\hbar/\sqrt{m\epsilon})/\sigma$, which effectively measures the quantum delocalization of the wave functions relative to the system scale defined by σ. For most other pair potentials (e.g., the Morse potential), in addition to the quantum parameter, one has to specify at least one other parameter. This makes the LJ system a good choice for systematic studies of quantum effects, while minimizing the numerical work.

The thermodynamics of LJ clusters is both very complex and numerically challenging even without taking into account the quantum effects (see, e.g., Refs. [1–5]), while including the quantum effects increases both the algorithmic complexity and computational cost by orders of magnitude. Some recent examples are Refs. [6–9].

The two dominant structural types that are realized in the classical limit ($\Lambda=0$) for global energy minima of all clusters (except some special cases, such as LJ_{38}) are based on either the Mackay icosahedral or anti-Mackay (or polyicosahedral) motifs, which correspond, respectively, to an incomplete Mackay or anti-Mackay overlayer surrounding a Mackay icosahedral core [10–13]. The atoms in an anti-Mackay overlayer are more loosely packed than in a Mackay overlayer and as such have more liquidlike character. (Note, however, that in some cases an anti-Mackay structure could also be characterized as solidlike as it may still be highly symmetric.) For $n=31,\ldots,55$, the Mackay packing is energetically more favorable than the anti-Mackay one. However, heating of a cluster with the Mackay global minimum may induce a transition to an anti-Mackay structure, because the latter is entropically more favorable than the former [3,5]. For the special case of LJ_{38}, which has an octahedral global minimum, the "solid-solid" thermally induced transition takes place [1,2] due to the fact that the octahedral structure is entropically less favorable than the Mackay structures. Further heating of the cluster would result in the Mackay $\rightarrow$anti-Mackay (M$\rightarrow$aM) transition similar to those that occur in the other clusters with the Mackay global minimum. References [8,9] report results for Ne_n clusters, which show that the quantum delocalization ($\Lambda=0.095$), just like heating, can make the anti-Mackay packing energetically most favorable. In addition, Ref. [9] shows that none of the nonicosahedral ground states survive for sizes up to $n=147$.

In the present study, we estimate the ground states (i.e., zero temperature) of the LJ_n clusters with sizes $n=31,\ldots,45$ for the range of quantum parameter $\Lambda\in[0;0.3]$. We note here that examples of such studies can be found in the literature. In Ref. [14], Calvo *et al.* in particular used the harmonic approximation (HA) to investigate the relative stabilities of ground-state structures for LJ clusters for a set of Λ values corresponding to xenon ($\Lambda=0.01$), argon ($\Lambda=0.03$), and neon ($\Lambda=0.095$). They indicated that the anti-Mackay structure may become more energetically favorable than the Mackay one when Λ is sufficiently large. Later, Doye and Calvo [15] used the HA to determine the ranges of stability of competing structural motifs (namely, icosahedral, decahedral, and fcc) as a function of size and quantum parameter for large "magic-number" clusters. While the HA may be adequate for nearly classical cases, such as, e.g., xenon and argon, as shown in Ref. [8], and also in the present work, in a more quantum regime, e.g., corresponding to neon, the HA is not quite accurate. More recently, Derrickson and Bittner [16] applied a Bohmian hydrodynamic approach to estimate the ground states of several small argon and neon clusters. There is an indication, however, that the latter method may even yield unphysical results [17].

Our method of choice for the estimation of cluster ground states is based on the use of the variational Gaussian wave packets (VGWs) [7–9]. A VGW gives the exact ground state for a harmonic potential. While it is manifestly approximate for a general anharmonic potential, the VGW method demonstrated its practicality, specifically, for the case of Ne_{38} (see Ref. [8]), for which the VGW energies agreed very well with those computed by the path-integral Monte Carlo (PIMC) method.

A VGW,

$$\langle r|q_0;\tau\rangle = \exp\left[-\frac{1}{2}(r-q)^{\mathrm{T}}G^{-1}(r-q)+\gamma\right], \qquad (2)$$

is an approximation to the solution of the imaginary-time Schrödinger equation $|q_0;\tau\rangle \approx e^{-\tau\hat{H}}|q_0;0\rangle$ with the initial condition $\langle r|q_0;0\rangle = \delta(r-q_0)$. The VGW is propagated in the imaginary time τ by solving a system of coupled ordinary differential equations for the time-dependent parameters $G=G(\tau)$, $q=q(\tau)$, and $\gamma=\gamma(\tau)$ corresponding, respectively, to the Gaussian width matrix (a $3n\times 3n$ real symmetric and positive-definite matrix), the Gaussian center (a real $3n$ vector), and a real scale factor. In the zero-temperature limit ($\tau\to\infty$), the VGW becomes stationary and minimizes the energy functional

$$E = \frac{\langle q_0;\tau|\hat{H}|q_0;\tau\rangle}{\langle q_0;\tau|q_0;\tau\rangle}. \qquad (3)$$

The VGW propagation in τ is made efficient by fitting the LJ potential by a sum of Gaussians,

$$U(r_{ij}) \approx \sum_{p=1}^{P} c_p \exp(-\alpha_p r_{ij}^2). \qquad (4)$$

In the present study, six Gaussians are used [18], which provides a slightly more accurate approximation for the potential than the three-Gaussian fit used in Refs. [7–9]. The parameters of the present Gaussian fit are

p	c_p	α_p
1	31279960.65933084	35.14249661727566
2	1668963.963961670	21.73050942017830
3	91092.34069670191	13.25329843520143
4	3354.805129558428	7.60982070333635
5	−8.46844309983970	1.67180258175699
6	−0.38418467585210	0.50261814095335

For a single-minimum potential, there is a single stationary VGW, while otherwise there may be multiple stationary VGWs, typically (albeit not always, if the minima are not deep enough [8]) one per minimum. The problem of finding the best estimate for the ground state then becomes akin to a global optimization. Here we adapt the procedure of Refs. [8,9]. For each cluster size, $n=31,\ldots,45$, long random walks are generated by the replica-exchange Monte Carlo method [19] using the corresponding classical system. Every once in 10^5 MC steps, the replica configurations with temperatures around the corresponding classical M→aM transition are quenched up to $\tau\sim 100$ (or $T\sim 0.01$ in reduced units), resulting in a nearly stationary VGW. The quenching is performed for the set of quantum parameters $\Lambda=\{0.095,0.19,0.30\}$. At the end of the simulation, the 20 different lowest-energy configurations for each of the above three Λ values are retained, resulting in a set of 60 configurations. Each of these 60 configurations q_0 is then quenched on a fine grid of the quantum parameter $\Lambda\in[0;0.32]$ by changing Λ incrementally and using the final value $q(\tau)$ of the quenched configuration as the starting point for the next value of Λ.

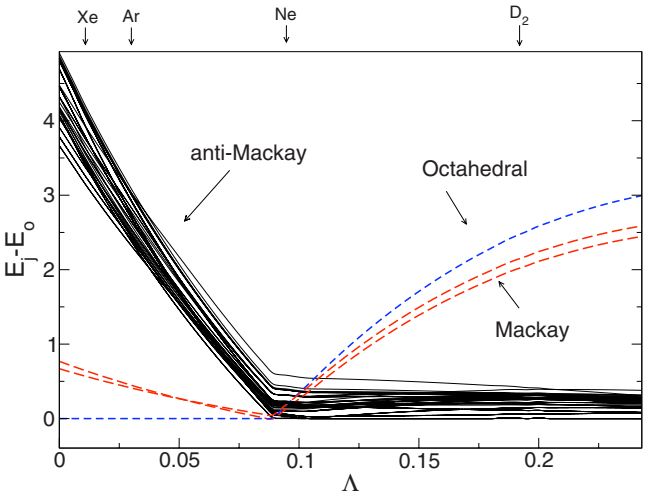

FIG. 1. (Color online) Energies of selected stationary Gaussians, $E_j(\Lambda)-E_0(\Lambda)$ [relative to the ground state energy $E_0(\Lambda)$], of LJ_{38} cluster as a function of the de Boer quantum delocalization parameter Λ for the octahedral, Mackay, and anti-Mackay configurations.

As an example, Fig. 1 shows energies $E_j(\Lambda)$ [relative to the ground state energy $E_0(\Lambda)$] as a function of Λ for the LJ_{38} cluster obtained by the procedure described above. In the classical regime, the octahedral and the Mackay structures are very close in energies while the anti-Mackay structures have substantially higher energies. Figure 2 shows the three energy curves, one for each of the three competing structural motifs. In order to make the figure easier to read, the energies are shown relative to the harmonic energy for the octahedral minimum. The most interesting range of quantum parameters corresponds to $\Lambda\in[0.086:0.09]$, where all three structural types have similar energies. Figure 3 shows the ground-state energy $E_0(\Lambda)$ for this range (also relative to

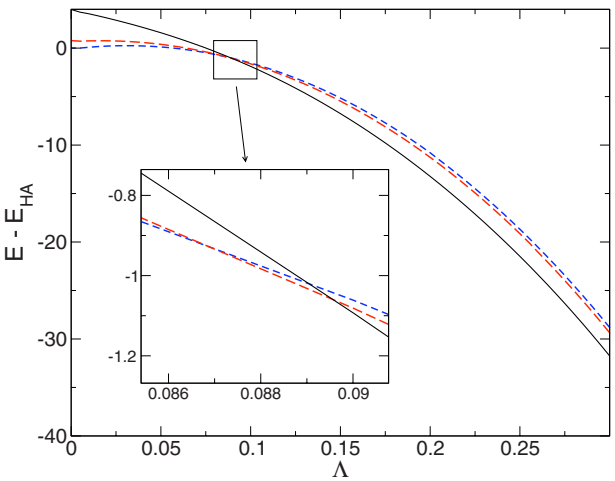

FIG. 2. (Color online) The VGW energies $E(\Lambda)-E_{\mathrm{HA}}(\Lambda)$ (after subtraction of the HA for the octahedral configuration) for the same configurations as in Fig. 4.

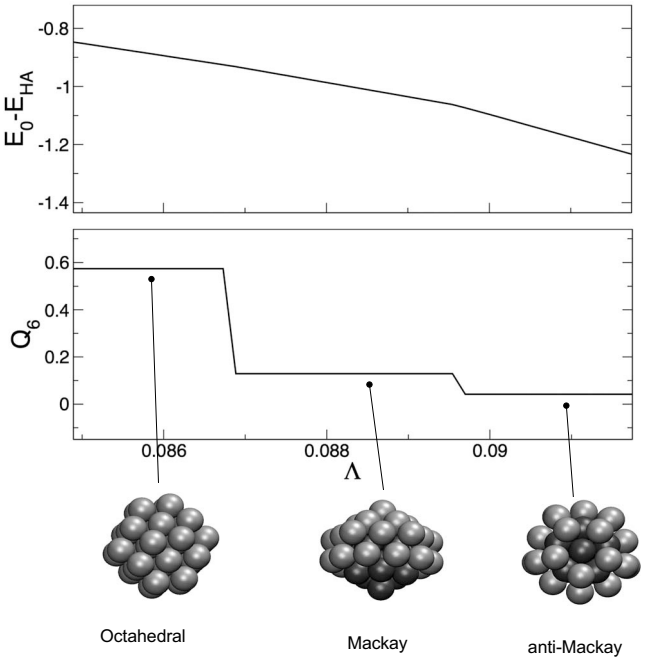

FIG. 3. The ground-state energy $E_0(\Lambda)-E_{\mathrm{HA}}(\Lambda)$ (after subtraction of its linear fit at $\Lambda=0$, i.e., the HA for the octahedral configuration) and the Q_6 orientational bond-order parameter for the LJ_{38} cluster as a function of the de Boer parameter Λ. Each of the three structures depicted in the figure is energetically favorable for a certain range of Λ.

the harmonic energy of the octahedral configuration), and $Q_6(\Lambda)$, the orientational bond-order parameter [20]. The latter is a convenient indicator of the structure. The three different structures are also depicted in the figure. The particularly interesting result of this calculation is that the octahedral configuration has the lowest energy for $\Lambda<0.0868$, the Mackay structure is energetically most favorable only over the narrow range $\Lambda\in[0.0868;0.0895]$, while the anti-Mackay structure has the lowest energy for $\Lambda>0.0895$.

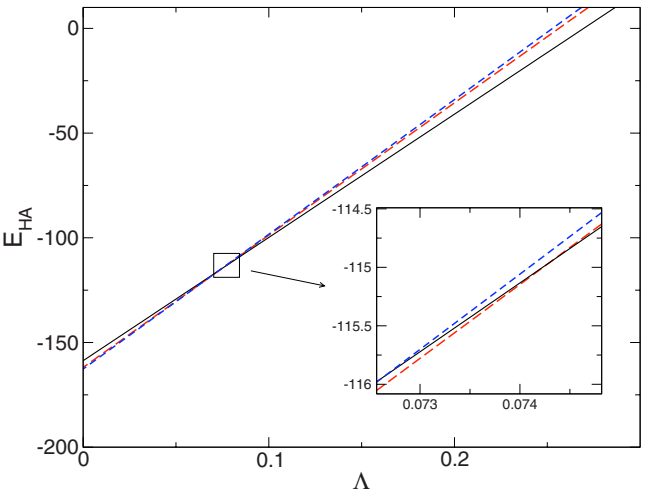

FIG. 4. (Color online) The HA energies E_{HA} as a function of the quantum parameter Λ for the three competing configurations of the LJ_{38} cluster, having the octahedral, Mackay, and anti-Mackay structures.

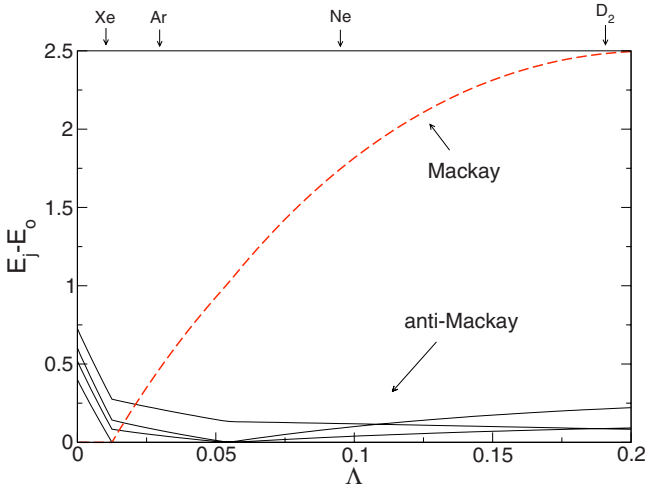

FIG. 5. (Color online) Same as Fig. 1 but for the LJ_{31} cluster.

In the $\Lambda\to 0$ limit, the HA becomes exact and as such coincides with the VGW result. However, the harmonic energies E_{HA} depend linearly on Λ as shown in Fig. 4 for the three competing configurations of the LJ_{38} cluster. The three straight lines merge for $\Lambda\sim 0.073$, which is quite different from the VGW result. Already for $\Lambda\sim 0.03$ (corresponding to Ar_{38}) the deviation of the VGW energies from straight lines is noticeable (see Fig. 2).

Figure 5 shows the energy diagram for LJ_{31}. The quenching analysis for this cluster resulted in only five different configurations, corresponding to the Mackay global minimum and four anti-Mackay local minima. The Mackay $\to$anti-Mackay transition occurs at $\Lambda\approx 0.012$, i.e., at a much lower value than that for LJ_{38}. This is not surprising since

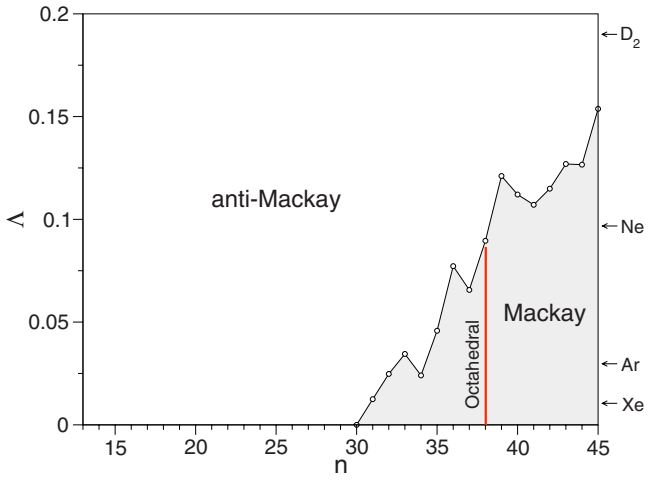

FIG. 6. (Color online) The "phase diagram" for LJ_n clusters displaying the ranges of stability of Mackay and anti-Mackay ground-state structures. For each cluster size n, the point indicates the value of the quantum parameter Λ at which the M$\to$aM transition occurs. The vertical line for $n=38$ indicates the stability range of the octahedral ground state.

LJ_{31} is the smallest two-layer cluster with a Mackay global minimum, the anti-Mackay local minimum being very close in energy to the latter. Also note that when Λ is increased further, the ground state switches to another anti-Mackay configuration.

We performed a similar analysis for all cluster sizes up to $n=45$ (where LJ_{45} is the largest cluster, for which an anti-Mackay structure exists). The results are summarized in Fig. 6 which shows the ranges of stability of the Mackay and anti-Mackay structures, with the LJ_{38} being a special case.

In conclusion, systematic analysis of size-induced ($T=0$) or temperature-induced ($n=$const) Mackay$\rightarrow$anti-Mackay structural transitions in LJ clusters has been reported previously. PIMC and VGW studies for particular quantum LJ clusters have also been reported previously, as well as studies based on the use of more approximate methods (such as the HA). The present work performs a systematic analysis of the ground-state structures as a function of both size n and the de Boer quantum delocalization length Λ. Our results are consistent with the commonly exploited idea that the quantum effects alone can induce structural transformations.

Although we believe that our results are reliable, at least for the weakly quantum regime (say, $\Lambda<0.1$), for large values of Λ we cannot be so sure, as in strongly quantum systems the wave functions are strongly delocalized, making the Gaussian approximation inadequate. Unfortunately, there is no simple way to either systematically improve the VGW approximation or assess its reliability, beyond the documented (favorable) comparisons with the PIMC results for some neon clusters [7,8]. Future calculations using PIMC-based methods may clarify this issue, although a blind search for the ground state using such methods may be too expensive. However, as demonstrated in Ref. [8], combining PIMC with the VGW can make it practical.

We are grateful to Florent Calvo for very useful discussions. Support from NSF Grant No. CHE-0414110 is acknowledged.

[1] J. P. K. Doye, M. A. Miller, and D. J. Wales, J. Chem. Phys. **110**, 6896 (1999); **111**, 8417 (1999).
[2] J. P. Neirotti, F. Calvo, D. L. Freeman, and J. D. Doll, J. Chem. Phys. **112**, 10340 (2000); F. Calvo, J. P. Neirotti, D. L. Freeman, and J. D. Doll, *ibid.* **112**, 10350 (2000).
[3] F. Calvo and J. P. K. Doye, Phys. Rev. E **63**, 010902(R) (2000).
[4] D. D. Frantz, J. Chem. Phys. **115**, 6136 (2001).
[5] V. A. Mandelshtam and P. Frantsuzov, J. Chem. Phys. **124**, 204511 (2006).
[6] C. Predescu, D. Sabo, J. D. Doll, and D. L. Freeman, J. Chem. Phys. **119**, 12119 (2003); D. Sabo, C. Predescu, J. D. Doll, and D. L. Freeman, *ibid.* **121**, 856 (2004).
[7] P. Frantsuzov and V. A. Mandelshtam, J. Chem. Phys. **121**, 9247 (2004).
[8] C. Predescu, P. A. Frantsuzov, and V. A. Mandelshtam, J. Chem. Phys. **122**, 154305 (2005).
[9] P. A. Frantsuzov, D. Meluzzi, and V. A. Mandelshtam, Phys. Rev. Lett. **96**, 113401 (2006).
[10] J. A. Northby, J. Chem. Phys. **87**, 6166 (1987).
[11] J. P. K. Doye, D. J. Wales, and R. S. Berry, J. Chem. Phys. **103**, 4234 (1995).
[12] R. H. Leary, J. Global Optim. **11**, 35 (1997).
[13] D. J. Wales and J. P. K. Doye, J. Phys. Chem. A **101**, 5111 (1997).
[14] F. Calvo, J. P. K. Doye, and D. J. Wales, J. Chem. Phys. **114**, 7312 (2001).
[15] J. P. K. Doye and F. Calvo, J. Chem. Phys. **116**, 8307 (2002).
[16] S. W. Derrickson and E. R. Bittner, J. Phys. Chem. A **110**, 5333 (2006).
[17] S. W. Derrickson and E. R. Bittner, J. Phys. Chem. A **111**, 10345 (2007).
[18] P. Frantsuzov and V. A. Mandelshtam, J. Chem. Phys. **128**, 094304 (2008).
[19] C. J. Geyer, in *Computing Science and Statistics: Proceedings of the 23rd Symposium on the Interface*, edited by E. M. Keramigas (Interface Foundation, Fairfax, VA, 1991), pp. 156–163; K. Hukushima and K. Nemoto, J. Phys. Soc. Jpn. **65**, 1604 (1996).
[20] P. J. Steinhardt, D. R. Nelson, and M. Ronchetti, Phys. Rev. B **28**, 784 (1983).